DEVELOPMENT THE ELECTRONIC SYSTEM OF CONTINUES MODULAR SNAKE-LIKE-ROBOT

DANIEL ARMANDO GÓMEZ, JAVIER CAMILO TORRES VERA
El Bosque University, Electronics Engineering Department
Av. Cra 9 No. 131 A – 02 Bogota, Colombia

HERNANDO LEÓN-RODRÍGUEZ
El Bosque University, Electronics Engineering and Bioengineering Department
Av. Cra 9 No. 131 A – 02 Bogota, Colombia

This project consists of the development of an electronic system to manipulate a snake like robot in a modular way. The electronic cards were implemented in a master-slave relationship for joint control of each mechanical module. These cards are composed of a DSPic30F4011, microchip 16-bit microcontroller that incorporates the CAN module, essential protocol for communication between cards, PWM outputs for motor control, analogue and digital ports; as well as a socket to connect to an external device through the UART. The firmware has been written in MikroC Pro. Each microcontroller implements the characteristic equation from the Hirose curves to generate a serpentine movement. These moves were simulated using ROS (Robotic Operating System in Rviz).

1. Introduction

The structural design of a snake is based on the repetition of its spine along its entire body, where only 3 types of bones make it up: the skull, the vertebrae and the ribs. The vertebral column is composed of between 100 and 400 vertebrae and each vertebra allows small movements in vertical and lateral direction, but the composition of so many vertebrae allows the snake a great flexibility and curvature with dramatically large forces.

The anatomy of the snake is composed of the same type of union and structure where each vertebra allows a rotation in the horizontal plane of 10-20 degrees and a rotation between 2-3 degrees in the vertical plane. [1] The locomotion system of the snake is very stable and the body is in constant contact with the ground at different points, allowing a low centre of mass and great traction which is easy to perceive its great ability with low energy consumption.

Snake-inspired robots were introduced in the 1970s by Shigeo Hirose. [2] Since then, several numbers of bio-inspired designs about snake like robots have been conceived and constructed. Although, the numerous designs of robots follow the kinematics and locomotion imitating the snake, they can change enormously in their physical configuration and purpose. For example, some robots are redundant; others are hyper-redundant while others may not have redundancy at all. [3] The first designs of snake-robots used traction wheels or tracks, while at present they can use passive wheels or without wheels at all. [4] Some designs are amphibious and can move effortlessly between terrestrial environments and water. [1] [6] [8] However, the demand for new types of

H. Montes et al. (eds.), *CLAWAR 2018: 21st International Conference on Climbing and Walking Robots and the Support Technologies for Mobile Machines*,
Robotics Transforming the Future

robots is still present for rescue and inspection applications, where they do not require a robot capable of negotiating such conditions and difficulties in sewer lines, water networks and swamps. Robots based on thin and flexible snakes meet some of these needs. [5][7][9][15]

Commercially, robots for exploration of pipes are of many kinds, where each one of them fulfils different functions, mainly visual inspection of pipelines of drinking water and hydro-sanitary lines through video capture. [16][17][18] However, these robots have a very large disadvantage, the most of them require a very expensive and heavy transport logistics and for inspection services where the cost of using this equipment makes its frequent application difficult.

Figure 1: Conceptual design and module of snake like robot.

Figure 1 shows the conceptual design of the modular snake scalable robot; it is composed by 7 modules each one adapted by 2 degrees of freedom, generated by two servomotors. In this sense, the electronic design is focused in a modular way so that each mechanical joint carries its electronic backup and battery.

2. Serpentine Locomotion

There are different types of locomotion in snakes based on the condition of the terrain and the type of environment. In the development of the project the cards and control can reproduce any of the 4 types of snake locomotion; however, the applications of the control system and the communications of the cards focused the serpentine locomotion, as verification of control system. [10]

3. Design of the electronic system

The conditions of the electronic design are based on the components necessary to generate the movement of the robot based on its locomotion, environment, size, current and application.

3.1. *Power requirement and voltage regulation*

The selected batteries are based on the power delivered, charging time and the space gap within of the modules. The selected batteries are lithium-polymer 72x34x14 mm 1000 mA, composed of two cells of 7.4 volts.

Due to the high efficiency of buck step-down type regulators, table 1 is showing the characteristics of the following devices that have been selected to satisfy current requirements of approximately 2.5 Amps, efficiency of 85% to 95%, capable to inverse voltage, and smaller as possible.

3.2. *Microcontroller and communication protocol*

The microcontroller that has been chosen mainly based on its 16-bit architecture; additionally, it has CAN communication protocol incorporated as a final purpose of control and position of the servomotors. Its parameters are: architecture:16-bits, CPU speed 30 MPS, type of minority: flash, memory: 48 KB, ram: 2 KB, temperature range 40 to 125 C, operating voltage 2.5 to 5.5 V, Number of I/O ports: 40, digital communication peripherals: 2-UART, 1-SPI; 1-I2C, analogue peripherals: 1-A/D, 9x10-bits; 1000 kps, communication protocol: CAN, PWM channels: 6 and parallel port: GPIO.

The proposed network protocol for internal communication between the electronic systems is a master-slave connexion. At the beginner, was considered to be performed through RS485, however, the CAN Bus was chosen, used in the automotive industry due to its robust protocol, which corrects transmission errors and It is invulnerable to electromagnetic disturbances, thanks to its physical layer requirements that are a shielded in a differential pair.

4. Mathematical analysis

Based on the cinematic analysis of Professor Hirose; [2] the behaviour and locomotion of a snake expresses the serpenoid curves and their joint trajectories as follow: [1] [2] [10] [14]

4.1. Serpenoidal Curves -Hirose

The following equations express the serpenoid curves proposed by Hirose. The length of the segment along the serpent is represented; a, b and c are parameters that determine the shape of the curve.

$$X(s) = \int_0^s \cos(a\ \cos b\sigma + c\sigma)\, d\sigma \tag{1}$$

$$Y(s) = \int_0^s \sin(a\ \cos b\sigma + c\sigma)\, d\sigma \tag{2}$$

4.2. Articular trajectories

The joint trajectories determine the angles that the joints must develop over time to generate a serpenoid curve; these equations are those which are executed by the microcontrollers on each electronic card in order to control the angles of the servomotors. The equation (3) contains a new component ω, which is determined by 2πf, where f is the frequency with the curve generated by equations (1) and (2).

$$\emptyset_i(t) = 2\alpha\ \sin(\omega t + (i-1)\beta) + \gamma \tag{3}$$

Where: (4), (5) and (6) come from the same parameters a, b and c of the serpenoid curve, [11]

$$\beta = \frac{b}{n} \tag{4}$$

$$\gamma = \frac{-c}{n} \tag{5}$$

$$\alpha = 2a\left|\sin\left(\frac{\beta}{2}\right)\right| \tag{6}$$

As a result: i, is the number of the joint, that is, the first joint will have an equation with $i = 1$, the second with $i = 2$ and so on.

5. Analysis and results

5.1. *Electronics card*

The figure 2 showing the electronic card implemented in each mechanical module of the robot structure. This card execute the master or slave control condition; the result is been done with a single card design allows to be configured as a master or slave according to the needs. Each card is identified with an internal code that permits to know its location on the robotic structure.

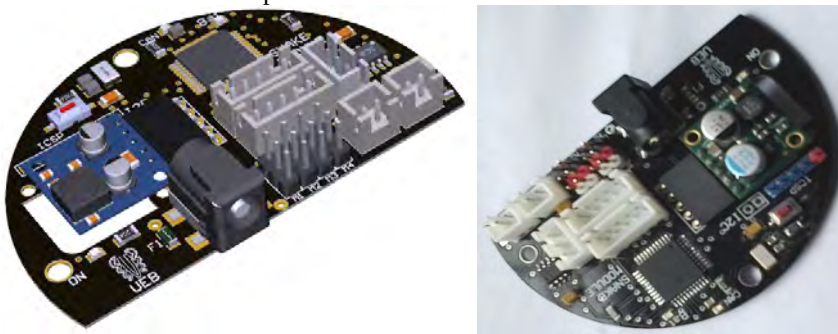

Figure 2: photorealistic image and picture of the developed control card.

The control and communication system of the developed card is presented in figure 3; this shows the diagram of any device with 5V supply voltage and logic, such as RF, Bluetooth, wifi modules that support the TTL/UART

interface. The diagram also showing the following the communication protocols: CAN; Uart, I2C that allow controlling any device such as sensors, servomotors, LEDs, etc. all them that support at the same time by the interface.

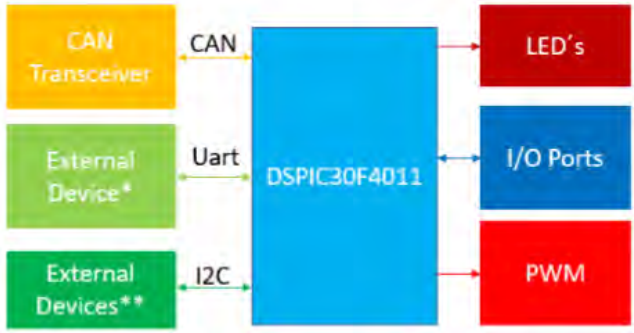

Figure 3: Block diagram of the electronic card.

5.2. *Mathematical analysis*

Figure 4-left is showing multiple serpenoid curves generated by the modification of different parameters in control, such as: frequency, amplitude and phase shifting.

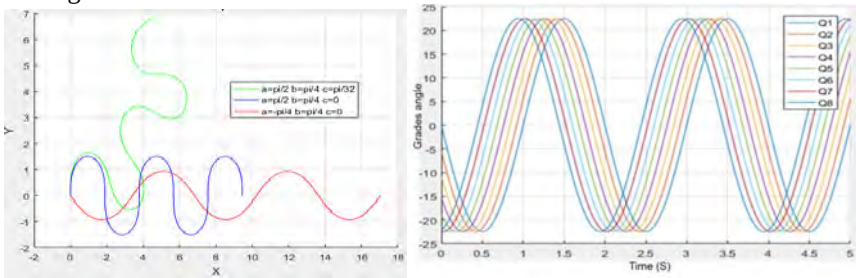

Figure 4: left: Simulation of trajectory behaviour and locomotion of the modular snake-robot; right: Articular angles with respect to time: left: a=-pi/4, c=pi/2, w=2pi*(0.5).

Figures 4-right is showing the simulations of each joint of the robotic system covering the joint angles (Q1 to Q8) with respect to time with different parameters *a*, *b* and *c*, based on equations 1 and 2.

Figure 4-right also showing the path of each of the joint modules to complete the serpenoid curve; it should be notice that if these graphs were developed with n=7, (number of joints) the results are similar.

6. Simulation of robot kinematics

The simulation includes the implementation of the joint trajectories in the mechanical modules of the robot. As a result, the robot design has been taken to

the URDF format compatible by the RVIZ simulator and through the publisher and subscriber of ROS. The described angles previously and the equations produce the simulated trajectories on RVIZ [12] [13].

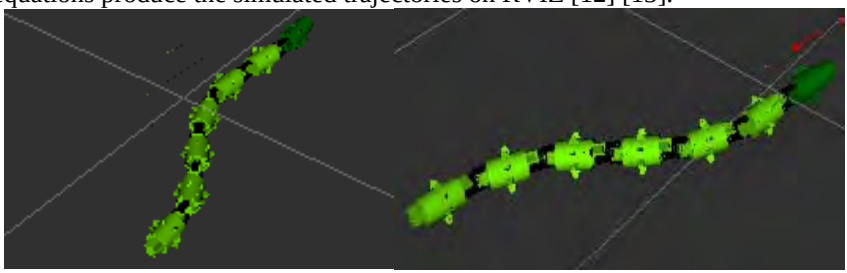

Figure 5: Result of robot simulation developing serpenoid curve in RVIZ-ROS.

The figure 5 is showing the executed simulation in RVIZ, in addition is validating that the robot could move in a serpentine way. However, in this first implementation, aspects such as the weight of the robot, friction and floor uniformity were not considered.

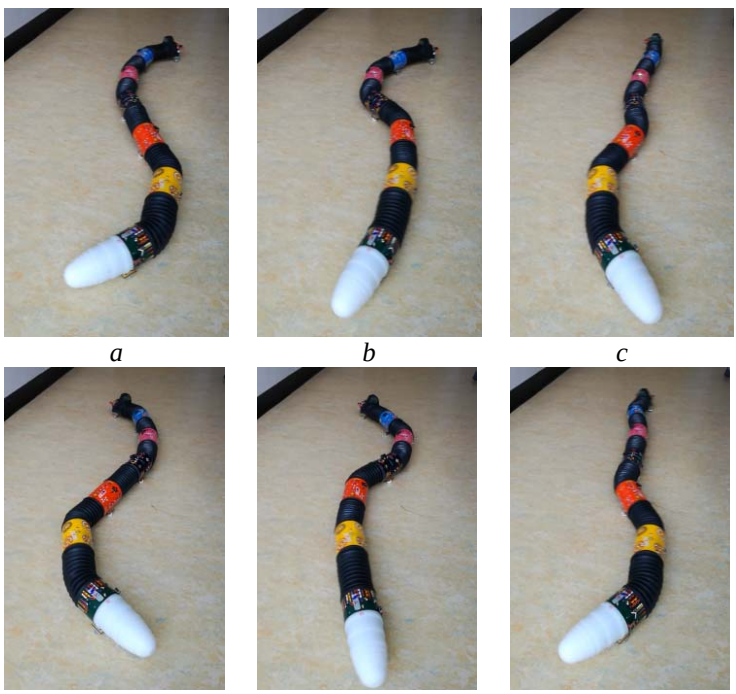

Figure 6: Motion sequence of the implemented robot like snake.

Figures 6 are showing the final implementation of the locomotion by the snake like robot based on the serpentine movements. Further research and word need

to be done in other to improve and produce soft-motion and better performance. Nevertheless, the control cards with CAN communications were well executed by the controllers, which were the aim of this preliminary research.

Conclusions

This project presents in a superficial way the design criteria for a particular electronic system to control a robot, these must cover its processing unit such as the microcontroller, its power supply and regulation, the peripherals that must be contemplated, either that you want to use sensors. Follow the rules as those established in IPC-2221 to develop PCBs with high quality standards.

The project presents the importance of a mathematical analysis in terms of robotics and its respective simulation to check its effectiveness. However, there is a huge gap between the simulation and the real, since some physical variables did not contemplated precisely.

Acknowledgment

This project openly thanks the contributions for the development of the control cards by the researchers: Michael Canu, Cecilia Murrugara; and especially to the Researcher Juan David Hernández of the University of Girona for his valuable contribution and knowledge in the management and control of ROS.

References

1. J. K. Hopkins, B.W. Spranklin, and S.K. Gupta, A survey of snake-inspired robot designs. Bioinspiration and Biomimetics, 4(2):021001, 2009.
2. S. Hirose and H. Yamada, Snake-Like Robots, Machine Design of Biologically Inspired Robots, IEEE Robotics & Automation Magazine, March 2009
3. K. J. Dowling, Limbless Locomotion: Learning to Crawl with a Snake Robot, The Robotics Institute Carnegie Mellon University and NASA Graduate Fellowships, December 1997.
4. S. Sugita, K. Ogami, G. Michele, S. Hirose, and K. Takita, A Study on the Mechanism and Locomotion Strategy for New Snake-Like Robot Active Cord Mechanism–Slime model 1 ACM-S1, Journal of Robotics andMechatronicsVol.20 No.2, 2008.
5. C. Wright, A. Buchan, B. Brown, J. Geist, M. Schwerin, D. Rollinson, M. Tesch, and H. Choset, Design and Architecture of the Unified Modular Snake Robot, 2012 IEEE International Conference.

6.S. Yu, S. Ma, B. Li, Y. Wang, An Amphibious Snake-like Robot: Design and Motion Experiments on Ground and in Water, Proceedings of the 2009 IEEE International Conference on Information and Automation, June 22 - 25, 2009, Zhuhai/Macau, China.
7. A. A. Transeth, R. I. Leine, C. Glocker and K. Y. Pettersen, 3D Snake Robot Motion: Nonsmooth Modeling, Simulations, and Experiments, IEEE transactions on robotics, vol. 24, no. 2, April 2008.
8. H. Yamada and S. Hirose, Study of a 2-DOF Joint for the Small Active Cord Mechanism, 2009 IEEE International Conference on Robotics and Automation Kobe International Conference Center, Kobe, Japan, May 12-17, 2009.
9. A.J. Ijspeert and A. Crespi; Online trajectory generation in an amphibious snake robot using a lamprey-like central pattern generator model, Proceedings of the 2007 IEEE International Conference on Robotics and Automation (ICRA 2007), pages 262-268,
10. David Rollinson; Control and Design of Snake Robots; School of Computer Science Carnegie Mellon University, 2014.
11. C. Gong, M. J. Travers, H.C. Astley, L. Li, J. R. Mendelson, D. I. Goldman and H. Choset; Kinematic gait synthesis for snake robots; The International Journal of Robotics Research 1–14, 2015
12. Filippo Sanfilippo, Øyvind Stavdahl and Pal Liljeback; SnakeSIM: A Snake Robot Simulation Framework for Perception-Driven Obstacle-Aided Locomotion; Proceeding of the 2nd International Symposium on Swarm Behavior and Bio-Inspired Robotics (SWARM), Kyoto, Japan, 2017.
13. F. Sanfilippo, Ø. Stavdahl and P. Liljeback; SnakeSIM: a ROS-based Rapid-Prototyping Framework for Perception-Driven Obstacle-Aided Locomotion of Snake Robots; Proceeding of the IEEE International Conference on Robotics and Biomimetics (ROBIO 2017).
14. S. G. Danielsen; Perception-Driven Obstacle-Aided Locomotion for snake robots, linking virtual to real prototypes; Norwegian University of Science and Technology, 2017
15. Biorobotics laboratory; (2018, May 16). Retrieved from: http://biorobotics.ri.cmu.edu/projects/modsnake/
16. Rausch Electronics USA; (2018, May 20). Retrieved from: http://rauschusa.com/
17. Aries Industries; (2018, June 13). Retrieved from: http://www.ariesindustries.com/
18. Ibak; (2018, June 10). Retrieved from: http://www.ibak.de

BIO-INSPIRED QUADRUPED ROBOT FOR DETECTION CARBON DIOXIDE IN THE AIR

MARIA CAMILA ROJAS SUÁREZ, SANTIAGO NORIEGA ÁLVAREZ
El Bosque University, Electronics Engineering Department
Av. Cra 9 No. 131 A – 02 Bogota, Colombia

HERNANDO LEÓN-RODRÍGUEZ
El Bosque University, Electronics Engineering and Bioengineering Department
Av. Cra 9 No. 131 A – 02 Bogota, Colombia

Quadruped in comparison with the majority of others animals, it has the ability to access to any kind of environment where others living creatures or even humans can't access. Those bio-inspired attributes are taken into this project in order to design and develop a quadruped robot with the abilities to move in all kind of directions like ascend or descend, avoid obstacles, etc. Combining these skills of the quadruped animals with the ability of continuously monitoring the carbon dioxide, the results can be determinants. This paper presents the dynamic and kinematics model in addition with the measurement scheme of the carbon dioxide index, with the purpose of establish a mechanical sturdy device, which can be monitoring an important variable. As a result, we studied the movement of real animals, so we can define a suitable bio-mimetic model for our robot.

1. Introduction

Recently, human has wanted to replicate all kind of movement of animal. This effort on doing it allowed humans to reproduce robots for certain task instead of risk their lives. This kind of biomimetic replication can be employed in land mines task and exploration task [1]. Another important application of these robots is the incursion in dangerous environments, like contaminated places, or hostile landmarks. In this order of ideas, we decided that the applicative background of the robot is the measurement of the concentration of carbon dioxide, which is an important variable that can generate negative impacts if no measurement (and regulation) control is applied. Besides, the human beings can be, easily, exposed to these gases without notice it, with mortal consequences.

Since 90's researches begin to innovate the whole world with bio-inspired robot [2]. In 2008 bio-inspired robots became in an important instrument, with several ability of walking and climbing in all kind of surfaces [3] [4].

H. Montes et al. (eds.), *CLAWAR 2018: 21st International Conference on Climbing and Walking Robots and the Support Technologies for Mobile Machines*,
Robotics Transforming the Future

Nowadays, the majority of quadruped robots have exceptional abilities and advanced material to be developed. Other approaches have been employed in their developed of quadruped robots as example parallel mechanism [5], soft materials [6] self-folding [7], Origami [7], printable robots and so on.

Nevertheless, this paper presents a device based on quadruped robots with some basic features and different attributes and applications. See figure 1.

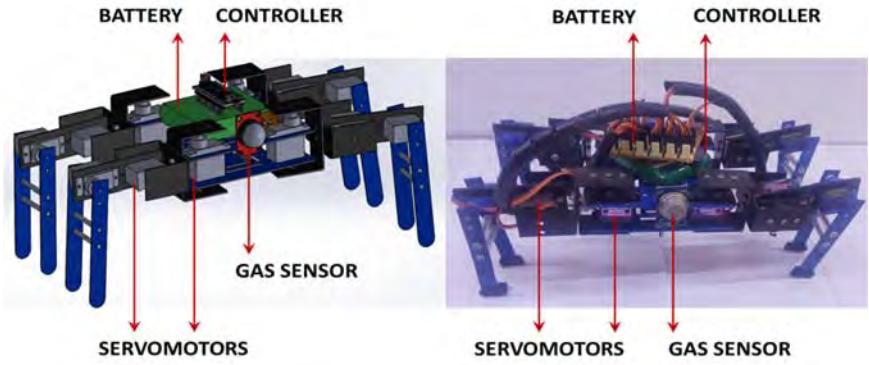

Figure 1: Quadruped robot design and prototype.

2. The Bio inspired quadruped and motion analysis

In order to accomplish this robot, we stablished how quadruped move and the algorithm behind this process. The majority of the quadrupeds move in a mammalian form, like a dog or a horse. Besides this, the spider has 8 limbs, so we couldn´t use them as a direct source of inspiration. To solve this problem, we used a mixture of sources of inspiration; we had the quadrupedal animals (their movement and behavior). On the other hand, we had the anatomy of the spider. As a result, the anatomy or physic shape of the spider, and the movement of the quadruped animals in an arachnid way was used.

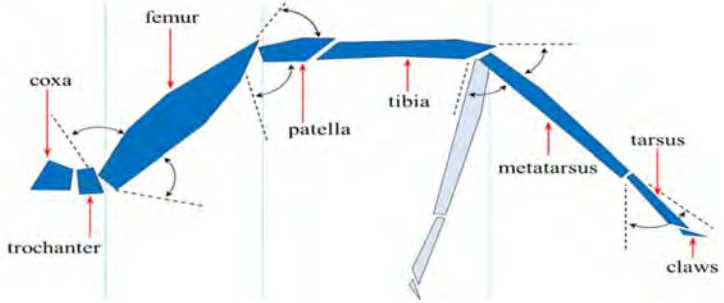

Figure 2: Spider’s leg biomechanics

Initially, it's important to know that the spider has 7 parts by leg (figure 2). From the original anatomy of the spider, we suppress some components that we didn't need. The reason of this is that we wanted to simplify the whole system. Having said this, instead of using the Patella part, we linked the femur and the tibia by a direct joint. The metatarsus and the tibia were united as a single link or part. Similarly, we dismiss the tarsus. All of these changes were executed in the robot, but for the kinematics analysis we took into account the entirely system for a realistic approach.

One important aspect is the amplitude that has every part of the spider's leg. This means, for example, that the coxa has amplitude of 35 degrees while tibia has a mobility of 70 degrees. Also, every of the seven components of the limb, has a different axis of movement; for example, the trochanter has a movement in X-Y axis, meanwhile the femur in X-Z axis. This kind of association and motion is explained graphically in the figure 2.

3. Mathematical development

As we mentioned previously, there are some constraints that we applied in the anatomic development. We applied these modifications in the mathematical development and we decided to involve all the possible variables, based on the following table to produces the most faithful model and prototype.

Table 1. Degrees and planes of work of each part of the quadruped robot.

Parts	Movements (degrees)	Plane
Coxa	75	Transversal
Femur	140	Sagittal
Tibia	40	Sagittal

3.1. *Direct Kinematics*

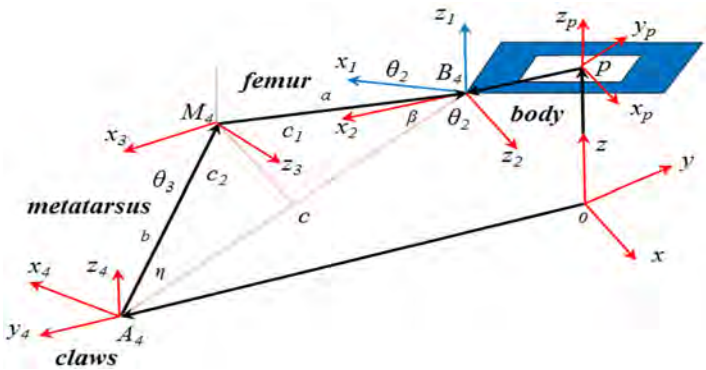

Figure 3: Parameters of the system and coordinate frames of the robot.

In order to study the direct kinematics of the robot was necessary, at the beginning; use the joint's variables of contact limbs and the position and orientation of the platform. All of this, based on fixed frame represented in figure 3. Is important to establish that the *Ai* vectors denote the end points of contact legs and the *Bi* vectors represent the connection points of the legs of the robot to the platform. Taking into account the figure 3 and knowing *Ai* vectors, which are the end points of contact legs, we can establish the next expression:

$$rBi = rAi + \frac{rMi}{Ai} + \frac{rBi}{Mi} \tag{1}$$

In this expression, rBi and rAi represent the position vector of *Bi*. In the same way, we needed to determinate all the parameters of the system in a graphically mean. In the figure 3 these parameters can be observed.

One highly important aspect in our robot was the motion and the sequence that a quadruped robot must follow in order to walk correctly. This item is the quadruped walking system, which is illustrated in the figure 4.

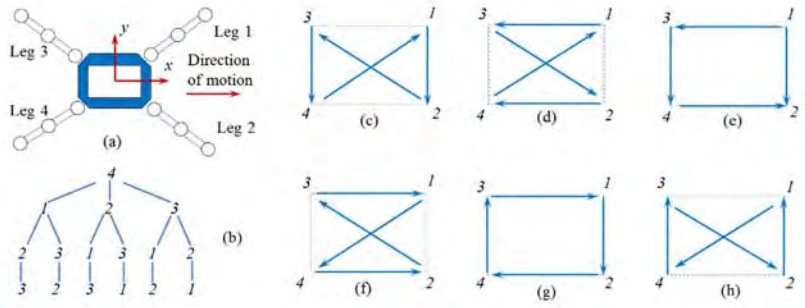

Figure 4: Sequence of quadruped walk

Suppose that the leg 1, 2 and 3 are standing on the ground. According to relation (1) the location of points *Bi* versus the fixed coordinate system are determined and, as direction of *x* axis of P-coordinate system is direct to $B3B1$ vector, is possible determine the direction of x-axis unit vector:

$$Ex = \frac{B3B1}{[\![B3B1]\!]} \tag{2}$$

In the same way, we can determinate the vector *B3B2*

$$Em = \frac{B3B2}{[\![B3B2]\!]} \tag{3}$$

By having this information, we can determinate the direction of unit vector, normal to the platform plane. To do this, we first need to implement the cross product of the two previous vectors:

$$Ez = EmxEx \tag{4}$$

In the same way, having the vectors *Ex* and *Ez*, is possible to determine the *Ey* vector using the same method:

$$Ey = Ex\ x\ Ez \tag{5}$$

These three vectors are necessary because we can establish the matrix of the platform versus the fixed coordinate system with the next expression:

$$^{P}_{B}R = [Ex\ Ey\ Ez] \tag{6}$$

In order to specify the origin of coordinate system, we can use the equation of the circle in this way:

$$(Xb1 - Xp)^2 + (Yb1 - Yp)^2 + (Zb1 - Zp)^2 = r^2 \tag{7}$$

$$(Xb2 - Xp)^2 + (Yb2 - Yp)^2 + (Zb2 - Zp)^2 = r^2 \tag{8}$$

$$(Xb3 - Xp)^2 + (Yb3 - Yp)^2 + (Zb3 - Zp)^2 = r^2 \tag{9}$$

If we solve the previously established equations system, we can determine the position of the body in the coordinate system.

3.2. *Platform velocity*

In order to establish the velocity of the robot's platform is necessary to determine the velocity and angular velocity of robot platform by using the position and velocity of the joint's variables. In order to specify the direct kinematics of platform velocity can use (10):

$$\overrightarrow{OA_i} + \overrightarrow{A_iM_i} + \overrightarrow{M_iB_i} + \overrightarrow{B_iP} = \overrightarrow{OP} \tag{10}$$

In the previous expression, *OAi* represents a vector that was drawn from the fix coordinate origin to point "A" from leg No. i. It's possible to determinate the relation between velocity of the joint's variables and platform velocity by differentiating from (10). The result is (11):

$$\vec{Vp} = {}^{B\to Tib}_{\omega_i} \times \vec{A_iM_i} + {}^{B\to Fem}_{\omega_i} \times \vec{M_iB_i} + {}^{B\to P}_{\omega} \times \vec{B_iP} \tag{11}$$

In (11), the first and third element of the equality represents the absolute angular velocity of femur and tibia, of limb No. i respectively. If we take into account the symmetry of our robot, (11) this process can be used for the other three contact legs. By using the fifth element of (11), is possible to establish *Vp*. Based on figure 3:

$${}^{1\to Tib}_{\omega_i} = \dot{\theta}_1 \vec{i}\vec{K}_1 + \dot{\zeta}\vec{i}\vec{K}_2 \tag{12}$$

$${}^{1\to Fem}_{\omega_i} = \dot{\theta}_1 \vec{i}\vec{K}_1 + \dot{\zeta}\vec{i}\vec{K}_3 \tag{13}$$

Regarding to the figure 3:

$$\zeta = \frac{\pi}{2} - \theta_2 - \theta_3 \rightarrow \dot{\zeta} = (\dot{\theta_2} + \dot{\theta_3}) \tag{14}$$

$$\gamma = \frac{\pi}{2} - \theta_2 \rightarrow \dot{\gamma} = -\dot{\theta_2} \tag{15}$$

In expressions (12) and (13), the first factor in both of them, indicates the unit vector direct to z-axis of first coordinate frame of limb No. i. The relation between the unit vectors of different coordinate frames of each leg is determined in function of the figure 3 as follow:

$$\overrightarrow{\iota_{K_3}} = \overrightarrow{\overrightarrow{\iota_{K_2}}} \tag{16}$$

$$\overrightarrow{\iota_{K_2}} = -\sin(\theta_1)\overrightarrow{\iota_{I_1}} + \cos(\theta_1)\overrightarrow{\iota_{J_1}} \tag{17}$$

$$\overrightarrow{\iota_{J_4}} = -\overrightarrow{\iota_{K_3}} \tag{18}$$

Using the expressions from (12) to (18), we can determine the values of ωi as follows:

$$^{1\rightarrow Tib}\omega_i = \dot{\theta}_1 {}^{i}\vec{K}_1 - (\dot{\theta}_2 + \dot{\theta}_3)(-S(\theta_1){}^{i}\vec{\imath}_1 + C(\theta_1){}^{i}\vec{\jmath}_1) \tag{19}$$

$$^{1\rightarrow Fem}\omega_i = \dot{\theta}_1 {}^{i}\vec{K}_1 - \dot{\theta}_2(-S(\theta_1){}^{i}\vec{\imath}_1 + C(\theta_1){}^{i}\vec{\jmath}_1) \tag{20}$$

In (19) and (20) the *S*'s and the *C*'s, means cosines and sines. In this case, for mathematical simplicity, we can express all the previous equations as rotational matrices as follows:

$$^{B\rightarrow Fem}\omega_i = {}^{P}_{B}R\ {}^{1}_{P}R_i\ {}^{1\rightarrow Fem}\omega_i \tag{21}$$

$$^{B\rightarrow Fem}\omega_i = {}^{1}_{B}R_i\ {}^{1\rightarrow Fem}\omega_i \tag{22}$$

$$^{B\rightarrow Tib}\omega_i = {}^{1}_{B}R_i\ {}^{1\rightarrow Tib}\omega_i \tag{23}$$

As we mentioned previously, *R* represents the rotational matrix of platform relative to the fix coordinate frame. In this order *R1p* is the rotation matrix of the first coordinate frame of limb No.i relative to P-coordinate frame system. This last rotational matrix is defined as follow:

$$R = \begin{bmatrix} \cos\left[(i-1)\frac{\Pi}{3} + \frac{\Pi}{6}\right] & -\sin\left[(i-1)\frac{\Pi}{3} + \frac{\Pi}{6}\right] & 0 \\ \sin\left[(i-1)\frac{\Pi}{3} + \frac{\Pi}{6}\right] & \cos\left[(i-1)\frac{\Pi}{3} + \frac{\Pi}{6}\right] & 0 \\ 0 & 0 & 1 \end{bmatrix} \tag{24}$$

3.3. *Direct kinematics of non-contact leg*

Direct kinematics of position for a non-contact limb is similar to the direct kinematics for a serial robot. As shown in Figure 3 can write:

$$OAi = OP + PBi + BiMi + MiAi \tag{25}$$

$$PBi = {}^{P}_{B}R\ PBi \tag{26}$$

$$BiMi = {}^{P}_{B}R\ {}^{1}_{P}R\ BiMi \tag{27}$$

$$MiAi = {}^{P}_{B}R\ {}^{1}_{P}R\ MiAi \tag{28}$$

Based on the previous expressions, *PBi* can be establishing as follows:

$$PBi = \begin{bmatrix} r\cos(\frac{\Pi}{6} + (i-1)\frac{\Pi}{6}) \\ r\sin(\frac{\Pi}{6} + (i-1)\frac{\Pi}{6}) \\ 0 \end{bmatrix} \quad (29)$$

As we did with the contact legs, we wanted to determine the velocity of the non-contact limbs, so the procedure is similar. We first need to differentiate (25) as follows:

$$\vec{V_{Ai}} = \vec{Vp} + \overset{B\to P}{\vec{\omega}} \times \vec{B_iP} + \overset{B\to Fem}{\vec{\omega_i}} \times \vec{B_iM_i} + \overset{B\to Tib}{\vec{\omega_i}} \times \vec{M_iA_i} \quad (30)$$

Using Vp and ω, that were derived from (11):

$$\overset{B\to Fem}{\omega_i} = \dot{\theta}_1 \dot{i}\vec{K_1} + \dot{\theta}_2 \dot{i}\vec{K_2} + \overset{B\to P}{\omega} \quad (31)$$

$$\overset{B\to Tib}{\omega} = \dot{\theta}_3 \dot{i}\vec{K_3} + \dot{\theta}_1 \dot{i}\vec{K_1} + \dot{\theta}_2 \dot{i}\vec{K_2} + \overset{B\to P}{\omega} \quad (32)$$

From (30) to (32) we can determine the velocity of end points of non-contact legs; as a result, these values can be specified.

4. Software and Carbon Dioxide Reading Sensor

The robot control was based in arduino controller and Bluetooth communication system, sending and receiving routine commands from mobile device. We used an Arduino-Nano as the controller for the full platform control and communication system. For motion, 12 servo-actuators were set, 3 for each leg with a torque of 2.2 kg.cm. These servo-motors are attached directly as a joint of each link-leg. The supply voltage and current for the robot was a battery package of 4.8 V and 3000 mA with around power of 7.5 W approx.

Regarding to the reading of the carbon dioxide index, an embedded circuit capable of monitoring various types of gases was implemented.

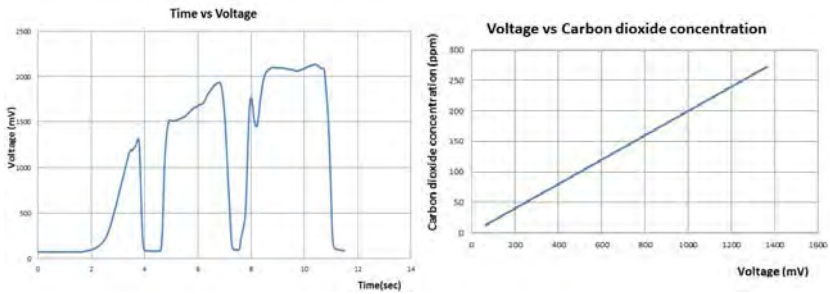

Figure 5: left: Response profile MQ4, time vs voltage; right: Voltage vs Carbon dioxide.

The figure 5-left shows the output voltage of the sensor depending of the gas concentration reading by itself. The result was obtained by adapting the gas

source next to the sensor; meanwhile the gas concentration was increasing.

Figure 5-right shows the relation of output voltage with the carbon dioxide concentration; in this way, the characterization of the sensor was adapted through a linear regression model, obtaining accurate results. An extremely important aspect to mention is the fact that this issue is still being evaluated and treated, with the purpose of implementing the sensor that best shapes to the context and conditioning with the purpose of achieving the best results.

5. Conclusions

The project has achieved systematically the design, development and control of a quadruped walking robot. The mathematical model helped out the modeling of the motion´s behavior of the robot. The robot has 12 DOF in total, 3 DOF for each leg, controlled by an Arduino Nano via a remote mobile device. The movement has been analyzed with biomimetic inspirations take from the spiders. The gas sensor MQ4 was an excellent first approach to the gas sensing technology because it allowed characterizing the behavior of the gas. Additionally, these results will serve us as a foundation in future research.

References

1. Z. Tang, P. Qi, J. Dai. (2017) "Mechanism design of a biomimetic quadruped robot", Industrial Robot: An Intl. Journal, Vol. 44 Issue: 4.
2. S. Shoval, E. Rimon and A. Shapiro, "Design of a spider-like robot for motion with quasi-static force constraints," Proc. 1999 IEEE Intl Conf on Robotics and Automation, Detroit, MI, 1999, pp. 1377-1383 vol.2.
3. Yi Lu, Keke Zhou, Nijia Ye, Design and kinemics/dynamics analysis of a novel climbing robot with tri-planar limbs for remanufacturing, J. Mech., Science and Tech., March 2017, Vol. 31, Iss. 3, pp 1427–1436
4. C. Semini, HyQ - Design and Development of a Hydraulically Actuated Quadruped Robot. PhD Thesis. April 2010.
5. H. Wang, Z. Qi, G. Xu, F. Xi, G. Hu and Z. Huang, Kinematics Analysis and Motion Simulation of a Quadruped Walking Robot with Parallel Leg Mechanism, The Open Mechanical Engineering Journal, 2010, 4, 77-85
6. M. Garabini, C.D. Santina, M. Bianchi, M. Catalano, G. Grioli, A. Bicchi (2017) Soft Robots that Mimic the Neuromusculoskeletal System. In: Converging Clinical and Engineering Research on Neurorehabilitation II. Biosystems & Biorobotics, vol 15. Springer, Cham.
7. C. D. Onal, M. T. Tolley, R. J. Wood, and D. Rus. Origami-Inspired Printed Robots; IEEE/ASME Trans. on Mech., Vol. 20, no. 5, Oct. 2015